

Partial Densities of States of Alloys Measured with X-Ray-Photoelectron Diffraction: AuCu₃(001)

A. Stuck, J. Osterwalder, T. Greber, S. Hüfner, and L. Schlapbach
Institut de Physique, Université de Fribourg, CH-1700 Fribourg, Switzerland
(Received 5 June 1990)

Using a single crystal of AuCu₃(001) as a test case, it is shown that x-ray-excited core-level-photoelectron-diffraction patterns of an ordered alloy can be employed to decompose the total alloy density of states of the valence band into the partial densities of states of the constituents. The results of this new method are in good agreement with earlier experiments and recent band-structure calculations. The ratios of core-level to valence-band cross sections of each constituent of the alloy are also determined and compared to those of the pure elements. Within experimental error no changes of these cross-section ratios upon alloying are observed.

PACS numbers: 79.60.Cn, 71.20.Cf

To understand the chemistry and physics of alloys, the partial valence-band densities of states (PDOS) of the constituents are of considerable importance. In the case of transition-metal alloys one can, with photoelectron spectroscopy as the measuring technique, exploit the different Cooper minima associated with *d* states, namely, the different energy dependences of the cross sections of the constituents, for a determination of the PDOS.¹ However, this elegant method suffers from some uncertainties. It assumes similar cross sections of the alloy and the corresponding pure metals for energies¹ between 20 and 200 eV and, in the case of single crystals, it neglects diffraction effects.

It is the purpose of this paper to show that it is instead possible to exploit differences in the angular dependences of the cross sections of each constituent at fixed energy in order to unfold the x-ray-photoelectron (XPS) valence-band (VB) spectra of alloys into the PDOS. Furthermore, we shall demonstrate that these angular cross-section variations can be measured very accurately by analyzing x-ray-photoelectron diffraction (XPD) of shallow core levels in the same crystal. No comparison with properties of pure metals is needed, since the diffraction patterns of the core levels of the alloy themselves serve as fingerprints for the constituents. The decomposition is independent of theoretically determined parameters and yields the PDOS and the ratio of the VB to the core-level cross sections for each element. These can be compared with results from other experiments or theories. DiCenzo *et al.*² and Citrin, Wertheim, and Baer³ used a similar approach to isolate the surface PDOS of Au and AuCu₃(001), respectively, but without taking into account final-state diffraction effects.

One of the most extensively studied alloys, AuCu₃, was chosen as a test case for the separation of the VB PDOS by XPD. Its electronic structure is reasonably well understood,⁴⁻⁶ and the band-structure calculations by Sohal *et al.*⁴ are in good agreement with photoemission experiments by the same authors.⁴ Nevertheless, Au-derived bands could only be found experimentally at binding energies larger than 5 eV while Wertheim¹ made

the interesting observation that the Au PDOS extends over the whole *d*-band region from 2- to 8-eV binding energy. A considerable hybridization of the Cu *3d* and Au *5d* bands was found in the calculations of the DOS in ordered and disordered AuCu₃.^{4,7}

XPD is by now a well established technique for studying surface atomic structures.⁸ The experiment consists of measuring the photoelectron current from an oriented single crystal with high angular resolution, either by varying polar and azimuthal angles at fixed photon energy or by measuring at fixed geometry as a function of photon energy. The observed intensity variations can be interpreted in terms of scattering and diffraction of the final-state photoelectron wave by the first few neighbor shells around the photoemitter. Structural conclusions can then be drawn by applying a scattering cluster theory.⁸ The valence bands and low-binding-energy core levels of simple metals have very similar diffraction patterns, as has recently been shown by Osterwalder *et al.* for Al(001).⁹ A localization of the photoemission hole state has been inferred to give rise to essentially the same scattering and diffraction of the photoelectrons originating from extended valence states as those from localized core levels. This similarity also holds for the VB of noble metals,^{10,11} at least as long as direct transitions are not important. As we shall demonstrate below, this is also true for the XPS measurements of AuCu₃(001) at 300 K.

In Fig. 1 we show the azimuthal core-level diffraction patterns from an AuCu₃(001) single crystal. Two shallow core levels, namely, Cu *3p* ($E_{\text{kin}} = 1177$ eV) and Au *4f* ($E_{\text{kin}} = 1167$ eV), were observed at a polar angle of $\theta = 54.7^\circ$ relative to the surface normal. The corresponding valence-band diffraction patterns, labeled VB I and VB II, are also given. They measure the intensities of the two prominent valence-band features (Fig. 2), which have previously been associated with predominantly Au (VB I) and Cu (VB II) character, respectively.^{1,4} The four diffraction curves are quite similar, yet they show small but significant differences, mainly near the [111] direction. The Cu *3p* intensity maximum in the

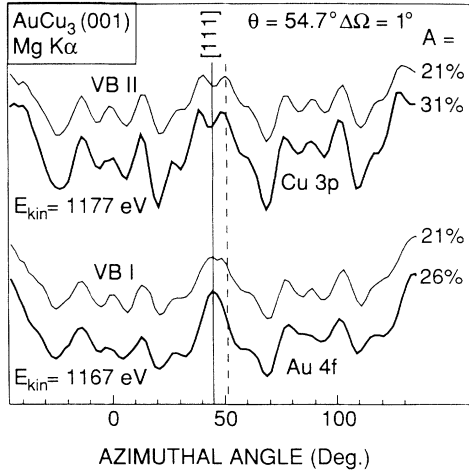


FIG. 1. Comparison of the Cu 3*p* and Au 4*f* core levels and associated VB diffraction patterns at $\theta=54.7^\circ$ off the surface normal. The lines indicate the azimuthal positions where different energy scans of the VB region (Fig. 2) were taken. Note the similar behavior of Au 4*f* and VB I scans and the VB II and Cu 3*p* scans in the vicinity of the [111] direction. In the case of the VB diffraction patterns the anisotropies are small because no background subtraction was used. The anisotropy A is defined as $(I_{\max} - I_{\min})/I_{\max}$, where I_{\max}, I_{\min} are, respectively, the maximal and the minimal intensities of the XPD pattern. It measures the strength of the diffraction.

[111] direction is split and has a local minimum at $\phi=45^\circ$ and two maxima at $\phi=39^\circ$ and 51° . In contrast, the Au 4*f* scan shows a single peak in the [111] direction. Similar and corresponding variations are found between the azimuthal scans of the two valence band regions, VB I and VB II. These qualitative differences clearly permit associating the VB I intensities predominantly with Au and VB II with Cu emission. Since even in the case of valence-band photoemission the final-state hole is well localized at the ion cores,⁹ these differences reflect the different local environments of each element in the ordered phase. In ordered AuCu₃(001) the top surface layer consists of 50% Cu and 50% Au while the second layer is pure Cu.¹² Subsequent layers alternate between these two types. Therefore, Au emitters are only present in every other layer, which we believe is the dominant factor for the differences in the diffraction patterns. Moreover, Au emitters have twelve Cu nearest neighbors while there are eight Cu and four Au nearest-neighbor atoms in the case of Cu. Consequently, the local scattering potential is different. Multiple-scattering calculations of the ordered alloy are under way.¹³

The combination of high kinetic energy (large k vector) and the low bulk Debye temperature of AuCu₃ (280 K) strongly favors indirect transitions.¹⁰ Thus, the whole Brillouin zone is sampled—a fact also known to be true for both Au and Cu.^{11,14} Therefore, our VB measurements should be sensitive to the PDOS, and little an-

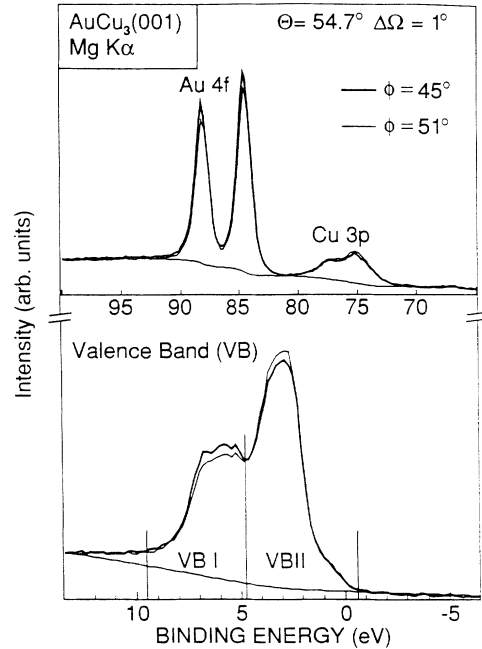


FIG. 2. Au 4*f* and Cu 3*p* core-level and valence-band spectra from AuCu₃(001) at two azimuthal angles $\phi=45.0^\circ$ and 51.0° , recorded at a fixed polar angle of $\theta=54.7^\circ$ off the surface normal. Diffraction-related intensity modulations of the two prominent VB features denoted as VB I and VB II are evident, associating VB I to predominantly Au and VB II to Cu emission. For the core-level spectra the Shirley background-subtraction procedure used in the data analysis is indicated.

gular variations due to direct transitions are expected. As mentioned above, the XPS VB photoemission process is localized. Neglecting the emission of valence s electrons,¹⁵ it can thus be assumed that the number of photoemitted VB electrons, $I^{\text{VB}}(\theta, \phi, E)$, measured at a given binding energy E and at angles θ, ϕ is a linear combination of Cu 3*d* and Au 5*d* contributions:

$$I^{\text{VB}}(\theta, \phi, E) = \sum_{i=\text{Au, Cu}} I_0 g_i^{\text{VB}}(\theta, \phi) \sigma_i^{\text{VB}} \frac{\rho_i^{\text{VB}}(E)}{n_i^{\text{VB}}}. \quad (1)$$

Here, the angular photoelectron distribution from the i th element ($i=\text{Au, Cu}$) is described by a diffraction function $g_i^{\text{VB}}(\theta, \phi)$, containing the angular dependence, I_0 is the photon intensity times the instrumental response, σ_i^{VB} is the total cross section of the VB d states of Au or Cu, $\rho_i^{\text{VB}}(E)$ is the PDOS as a function of binding energy, and n_i^{VB} is the number of d electrons of the i th element per unit cell. The VB cross sections are assumed to be constant as a function of binding energy. Any energy dependence of the cross sections is multiplied into the density of states $\rho_i^{\text{VB}}(E)$ and affects their shape. Likewise we can write for the energy-integrated intensities $S_i^{\text{core}}(\theta, \phi) = \int I_i^{\text{core}}(\theta, \phi, E) dE$ of the core-level peaks

$$S_i^{\text{core}}(\theta, \phi) = I_0 g_i^{\text{core}}(\theta, \phi) \sigma_i^{\text{core}}. \quad (2)$$

In the case of Al(001),⁹ the relative change in the wavelengths between Mg $K\alpha$ excited core and valence-band electrons is about 4.6%, while it lies between 3% and 3.5% for AuCu₃. In both cases, such small differences apparently have little effects on the interference patterns, as shown in Fig. 1. For AuCu₃, we can thus assume that the diffraction functions of the core and VB electrons are equal and therefore neglect any energy dependence of $g_i^{\text{VB}}(\theta, \phi)$, i.e., $g_i^{\text{VB}}(\theta, \phi) = g_i^{\text{core}}(\theta, \phi)$. Substituting Eq. (2) into Eq. (1) then yields

$$I^{\text{VB}}(\theta, \phi, E) = \sum_{i=\text{Au,Cu}} S_i^{\text{core}}(\theta, \phi) \frac{\sigma_i^{\text{VB}}}{\sigma_i^{\text{core}}} \frac{\rho_i^{\text{VB}}(E)}{n_i^{\text{VB}}} \quad (3)$$

and, after integrating over all energies $S^{\text{VB}}(\theta, \phi) = \int I^{\text{VB}}(\theta, \phi, E) dE$,

$$S^{\text{VB}}(\theta, \phi) = \sum_{i=\text{Au,Cu}} S_i^{\text{core}}(\theta, \phi) \frac{\sigma_i^{\text{VB}}}{\sigma_i^{\text{core}}}. \quad (4)$$

Measurements of the energy-integrated core-level and VB intensities for at least two different directions thus yield a set of linear equations [Eq. (4)], which can be solved for the ratios of the cross sections. Given these two ratios and the energy-resolved VB spectra, a second set of linear equations [Eq. (3)] at each energy channel remains which can be solved for the PDOS of the two elements. Both results, the cross-section ratios and the PDOS, are independent of experimental parameters such as the photon intensity and the instrumental response which cancel. They are furthermore independent of the stoichiometry of the alloy. This latter fact should allow the study of dilute systems. In AuCu₃ the absolute calibration of the PDOS was made by choosing $n_{\text{Au}}^{\text{VB}} = 10$ electrons/cell for Au and $n_{\text{Cu}}^{\text{VB}} = 30$ electrons/cell for Cu, once again neglecting s emission.

The experiments were performed with a modified VG ESCALAB Mark II spectrometer, equipped with a three-detector unit which enabled data accumulation with high angular resolution down to full acceptance cones of $\Delta\Omega < 1^\circ$. The angle between the k vectors of the x rays (Mg $K\alpha$, $h\omega = 1253.6$ eV) and the detected electrons is 54° . The sample was oriented with an accuracy of 1° and cleaned *in situ* by repeated cycles of 800-eV Ar⁺ sputtering and subsequent annealing up to 920 K. Further annealing cycles at 820 K were done until, at room temperature, sharp superstructure spots from LEED showed that the surface was well ordered. Small oxygen and carbon signals were still visible with XPS, corresponding to less than 10% of a monolayer of the contaminants. The stoichiometry was determined with XPS to be Cu:Au = 3 ± 0.5 . All data presented were measured at a fixed polar angle of $\theta = 54.7^\circ$ with respect to the surface normal and all energy spectra were numerically corrected for Mg $K\alpha$ satellites. A linear background subtraction was performed in every energy scan to obtain the core-level XPD as well as the total VB XPD patterns. The VB I and VB II XPD scans were

made without background subtraction. The background for all other VB spectra was calculated according to Steiner, Hoechst, and Huefner,¹⁶ using a Cu-like dielectric response function with a maximum at 20 eV. Linear, quadratic, and Shirley background-subtraction procedures were also used with no significant change in the form of the PDOS. The error bars for each PDOS were estimated to be 3 times the standard deviation of its points above the Fermi energy.

To illustrate the usefulness of Eqs. (3) and (4), we recorded core-level and VB spectra at two emission directions, as indicated in Fig. 1. In order to avoid any linear dependence within the sets of equations of type Eqs. (3) and (4) it is crucial that the diffraction functions for the two elements along the two chosen directions be different. That is, if we choose two or more directions for doing this decomposition over which $S_{\text{Au}}^{\text{core}}(\theta, \phi)$ is proportional to $S_{\text{Cu}}^{\text{core}}(\theta, \phi)$, then the two Eqs. (3) will not yield unique values for the PDOS. The resulting partial densities of states, as shown in Fig. 3, are in good agreement with both calculations by Weinberger and co-workers^{4,6} and the analysis by Wertheim.¹ This is in particular true for all peaks and the location of the minimum around 4 eV in the Au PDOS. The Au PDOS is low at the Fermi edge and has peaks at 2.4, 5.8, and 6.8 eV and a local minimum between 4 and 4.5 eV. The second main peak is more intense than the first one, which differs slightly from the interpretation of Wertheim,¹ but is in agreement with the calculations by

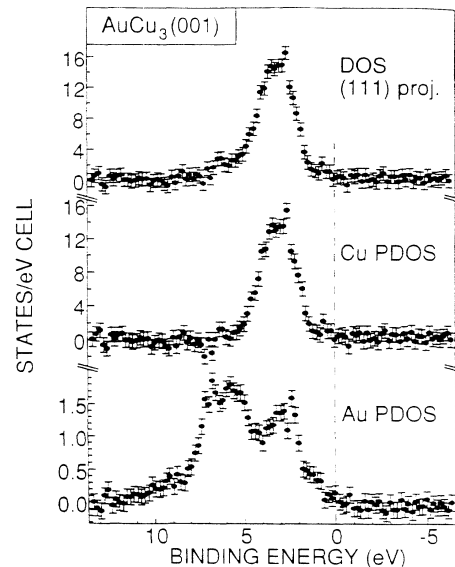


FIG. 3. Partial and total densities of states of AuCu₃(001), measured in the [111] direction and calculated with Eqs. (3) and (4). The absolute calibration of the PDOS was made by choosing $n_{\text{Au}}^{\text{VB}} = 10$ electrons/cell for Au and $n_{\text{Cu}}^{\text{VB}} = 30$ electrons/cell for Cu. For comparison with band-structure calculations, see Refs. 4 and 6.

Weinberger and co-workers.^{4,6} The peaks at 5.8 and 6.8 eV correspond to small oscillations in the XPS spectra, as shown in Fig. 2, and are even more pronounced in synchrotron-radiation^{4,5} and high-resolution XPS data.³

The Cu PDOS is flat between the Fermi energy and 1.4-eV binding energy and shows the dominant 3*d* band centered at about 3.2 eV with a FWHM of about 2.2 eV. Because of hybridization effects, a small Cu 3*d* contribution is predicted to appear between 5 and 6 eV.^{4,6} However, we do not find any significant Cu contribution in this energy region. The magnitude of the Cu PDOS peak of about 14 states/eV is in good agreement with the calculated value,^{4,6} whereas the magnitude of the Au PDOS is about 2–2.5 times too small. However, this difference is just due to our limited energy resolution which smears out the expected sharper peaks for Au, an effect also observed by Krummacher *et al.*¹⁷ The ratios of VB to core-level cross sections in AuCu₃, as calculated with Eq. (4), are 0.14 ± 0.02 for Au (core 4*f*) and 0.37 ± 0.06 for Cu (core 3*p*). As a reference, we also measured polycrystalline Au and Cu, giving cross-section ratios of 0.13 ± 0.01 for Au and 0.42 ± 0.02 for Cu. Within experimental error, no changes of the cross-section ratios upon alloying are observed. Thus, our initial assumptions are strongly supported.

At this point it is important to consider how unique the decomposition is with respect to the choice of pairs of emission directions. In photoemission from single crystals diffraction effects modulate not only the intensity but also the effective probing depth of the signal and our analysis always yields a combination of surface and bulk PDOS. This is of particular importance for Au emission from AuCu₃(001), as Au emitters are only present in odd layers. In order to get a predominantly bulklike Au PDOS one needs to measure along two closely spaced directions with at least some forward-scattering enhancement from subsurface Au layers, as is the case along [111]. The VB decomposition was also made with energy spectra taken at azimuthal angles of $\phi = 73^\circ$ and 87° , with θ still equal to 54.7° . These two directions are at least 10° away from any forward-scattering direction and the surface contribution should therefore be stronger. We find indeed an Au PDOS very similar to the Au surface density of states measured by DiCenzo *et al.*² Analogous to the case of pure metals,² decomposition of the surface and bulk PDOS contributions should be possible by comparing the PDOS and core-level intensities measured at different takeoff angles θ , but this is not attempted here. We also neglected angular changes of the VB cross sections due to the symmetry of the *d* shells, as discussed by McFeely *et al.*¹⁸

In summary, we have separated the PDOS of

AuCu₃(001) by using angular variations in x-ray-photoelectron spectra rather than the usual energy dependences of photoelectron cross sections. Consequently, no tunable synchrotron-radiation source is needed. Our results are in good agreement with calculations and earlier experiments, clearly demonstrating the validity of this novel method. Possible applications may include the study of insulators and epitaxially grown overlayers.

We would like to mention the skillful technical assistance of F. Bourqui, O. Raetzo, and H. Tschopp. We are also grateful to C. S. Fadley for critically reading this manuscript and to N. Montini for correcting our English. This work was supported by the Swiss National Science Foundation.

¹G. K. Wertheim, Phys. Rev. B **36**, 4432 (1987).

²S. B. DiCenzo, P. H. Citrin, E. H. Hartford, and G. K. Wertheim, Phys. Rev. B **34**, 1343 (1986).

³P. H. Citrin, G. K. Wertheim, and Y. Baer, Phys. Rev. Lett. **41**, 1425 (1978).

⁴G. S. Sohal, C. Carbone, E. Kisker, S. Krummacher, A. Fattah, W. Uelhoff, R. C. Albers, and P. Weinberger, Z. Phys. B **78**, 295 (1990).

⁵W. Eberhardt, S. C. Wu, R. Garrett, D. Sondericker, and F. Jona, Phys. Rev. B **31**, 8285 (1985).

⁶P. Weinberger, A. M. Boring, R. C. Albers, and W. M. Temmerman, Phys. Rev. B **38**, 5357 (1988).

⁷E. Arola, R. S. Rao, A. Salokatve, and A. Bansil, Phys. Rev. B **41**, 7361 (1990).

⁸C. S. Fadley, Phys. Scr. **T17**, 39 (1987); in "Synchrotron Radiation Research: Advances in Surface and Interface Science," edited by R. Z. Bachrach (Plenum, New York, to be published).

⁹J. Osterwalder, T. Greber, S. Hüfner, and L. Schlapbach, Phys. Rev. Lett. **64**, 2683 (1990).

¹⁰R. C. White, C. S. Fadley, M. Sagurton, and Z. Hussain, Phys. Rev. B **34**, 5226 (1986).

¹¹R. J. Baird, C. S. Fadley, and L. F. Wagener, Phys. Rev. B **15**, 666 (1977).

¹²T. M. Buck, G. H. Wheatley, and L. Marchut, Phys. Rev. Lett. **51**, 43 (1983).

¹³H. C. Poon, A. Stuck, J. Osterwalder, and L. Schlapbach (to be published).

¹⁴D. A. Shirley, J. Stoehr, P. S. Wehner, R. S. Williams, and G. Apai, Phys. Scr. **16**, 398 (1977).

¹⁵J. J. Yeh and I. Lindau, At. Data Nucl. Data Tables **32**, 1 (1985).

¹⁶P. Steiner, H. Hoehst, and S. Huefner, Z. Phys. B **30**, 129 (1978).

¹⁷S. Krummacher, N. Sen, W. Gudat, R. Johnson, F. Grey, and J. Ghijsen, Z. Phys. B **75**, 235 (1989).

¹⁸F. R. McFeely, J. Stöhr, G. Apai, P. S. Wehner, and D. A. Shirley, Phys. Rev. B **14**, 3273 (1976).